Acta Crystallographica Section B
Structural Science
ISSN 0108-7681

Disorder in Ag_7GeSe_5I, a superionic conductor: temperature-dependent anharmonic structural study

Stéphanie Albert,[a] Sébastien Pillet,[b] Claude Lecomte,[b] Annie Pradel[a]* and Michel Ribes[a]

[a]Institut Charles Gerhardt Montpellier, UMR 5253, CNRS Université Montpellier 2 CC 1503, Place E. Bataillon, F-34095 Montpellier CEDEX 5, France, and [b]Laboratoire de Cristallographie et de Modélisation des Matériaux Minéraux et Biologiques, UMR CNRS 7036, Nancy Université, BP 239, Boulevard des Aiguillettes, F-54506 Vandoeuvre-lès-Nancy CEDEX, France

Correspondence e-mail: apradel@lpmc.univ-montp2.fr

Received 20 June 2007
Accepted 15 November 2007

A temperature-dependent structural investigation of the substituted argyrodite Ag_7GeSe_5I has been carried out on a single crystal from 15 to 475 K, in steps of 50 K, and correlated to its conductivity properties. The argyrodite crystallizes in a cubic cell with the $F\bar{4}3m$ space group. The crystal structure exhibits high static and dynamic disorder which has been efficiently accounted for using a combination of (i) Gram–Charlier development of the Debye–Waller factors for iodine and silver, and (ii) a split-atom model for Ag^+ ions. An increased delocalization of the mobile d^{10} Ag^+ cations with temperature has been clearly shown by the inspection of the joint probability-density functions; the corresponding diffusion pathways have been determined.

1. Introduction

Superionic conductors have remarkable ionic mobility that induces conductivity in the solid state as large as that of the best liquid electrolytes, *i.e.* ranging typically from 0.01 to 1 Ω^{-1} cm^{-1}, and very weak activation energies for conductivity, *i.e.* ranging from 0.1 to 0.2 eV (Mahan & Roth, 1976). In all cases, these materials show high structural disorder in the mobile-ion sublattice. The most well known and most studied material in the family is probably AgI. The β phase, a poor conductor, stable at room temperature, transforms to the superionic α cubic phase with conductivity $\sigma \simeq 2$ Ω^{-1} cm^{-1} at 420 K. The two silver ions are statistically distributed over the 12 tetrahedral sites of the body-centred cubic cell (a = 5.602 Å, space group $Im\bar{3}m$, Z = 4) with large atomic displacement parameters related to a large anharmonic contribution (Wright & Fender, 1977). The superionic properties of α-AgI have encouraged a number of studies in the binary systems of the type AgI–MI, $M = K^+$, Rb^+, Cs^+ (Hull *et al.*, 2002). The aim was claimed to be the design of a material that would exist in its superionic form at room temperature and eventually below room temperature. The ternary compound $RbAg_4I_5$ was thus obtained. It crystallizes in a cubic space group ($P4_132$, Z = 4, a = 11.139 Å) with the I^- ions forming a β-Mn-type sublattice, while the Rb^+ ions are located in a distorted octahedral environment and the Ag^+ ions are statistically distributed over two tetrahedral sites of the I^- sublattice (Hull *et al.*, 2002). Its high ionic conductivity is the consequence of the statistical distribution of silver. Several other systems like α and α* Ag_3SI (Keen & Hull, 2001; Hull *et al.*, 2001) or Cu^+ conducting materials, such as γ-Cu_7PSe_6 (Gaudin *et al.*, 2000), exhibit similar behaviour.

The argyrodite compounds form an interesting family of superionic conductors. The term 'argyrodite' has been derived from the name of the natural compound Ag_8GeS_6. These ternary chalcogenides with the general formulation

Table 1
Summary of crystallographic data for Ag_7GeSe_5I.

Reliability factor: GOF = $\left(\Sigma w|F_{obs}^2 - F_{calc}^2|^2/(n-m)\right)^{1/2}$, $R(F) = \Sigma||F_{obs}| - |F_{calc}||/\Sigma|F_{obs}|$, $wR(F) = \left(\Sigma w||F_{obs}| - |F_{calc}||^2/\Sigma w|F_{obs}|^2\right)^{1/2}$ with $w = 1/\sigma(F)^2$ and $(n-m)$ degrees of freedom. $R_{int} = \sum_H \sum_i |I_{obs}^i - \bar{I}_{obs}|/\sum_H \sum_i \bar{I}_{obs}$.

	15 K	50 K	100 K	150 K	200 K
Crystal data					
Chemical formula	Ag_7GeSe_5I	Ag_7GeSe_5I	Ag_7GeSe_5I	Ag_7GeSe_5I	Ag_7GeSe_5I
M_r	1349.4	1349.4	1349.4	1349.4	1349.4
Cell setting, space group	Cubic, $F\bar{4}3m$	Cubic, $F\bar{4}3m$	Cubic, $F\bar{4}3m$	Cubic, $F\bar{4}3m$	Cubic, $F\bar{4}3m$
Temperature (K)	15	50	100	150	200
a (Å)	10.9558 (5)	10.9600 (7)	10.9683 (10)	10.9913 (4)	10.9955 (7)
V (Å^3)	1315.02 (10)	1316.5 (15)	1319.5 (2)	1327.8 (8)	1329.3 (15)
Z	4	4	4	4	4
D_x (Mg m^{-3})	6.823	6.815	6.799	6.757	6.749
Radiation type	Mo $K\alpha$	Mo $K\alpha$	Mo $K\alpha$	Mo $K\alpha$	Mo $K\alpha$
μ (mm^{-1})	28.3	28.3	28.3	28.3	28.3
Crystal form, colour	Block, black	Block, black	Block, black	Block, black	Block, black
Crystal size (mm)	0.08 × 0.08 × 0.04	0.08 × 0.08 × 0.04	0.08 × 0.08 × 0.04	0.08 × 0.08 × 0.04	0.08 × 0.08 × 0.04
Data collection					
Diffractometer	Xcalibur-Sapphire 2	Xcalibur-Sapphire 2	Xcalibur-Sapphire 2	Xcalibur-Sapphire 2	Xcalibur-Sapphire 2
Data collection method	ω scans	ω scans	ω scans	ω scans	ω scans
Absorption correction	Numerical	Numerical	Numerical	Numerical	Numerical
T_{min}	0.21	0.21	0.21	0.21	0.21
T_{max}	0.46	0.46	0.46	0.46	0.46
No. of measured, independent and observed reflections	2823, 412, 372	1222, 266, 259	4588, 332, 325	3451, 284, 277	4470, 336, 327
Criterion for observed reflections	$I > 2\sigma(I)$	$I > 2\sigma(I)$	$I > 2\sigma(I)$	$I > 2\sigma(I)$	$I > 2\sigma(I)$
R_{int}	0.058	0.040	0.071	0.056	0.062
θ_{max} (°)	39.2	32.3	35.6	32.5	35.8
Refinement					
Refinement on	F^2	F^2	F^2	F^2	F^2
$R[F^2 > 2\sigma(F^2)]$, $wR(F^2)$, S	0.060, 0.060, 5.35	0.047, 0.033, 4.78	0.055, 0.052, 5.72	0.047, 0.035, 5.20	0.059, 0.050, 4.93
No. of reflections	412	266	332	284	336
No. of parameters	41	36	36	39	38
Weighting scheme	Based on measured s.u.s, $w = 1/\sigma^2(I)$	Based on measured s.u.s, $w = 1/\sigma^2(I)$	Based on measured s.u.s, $w = 1/\sigma^2(I)$	Based on measured s.u.s, $w = 1/\sigma^2(I)$	Based on measured s.u.s, $w = 1/\sigma^2(I)$
$(\Delta/\sigma)_{max}$	0.021	0.013	0.024	0.007	0.006
$\Delta\rho_{max}$, $\Delta\rho_{min}$ (e Å^{-3})	6.22, −4.05	5.61, −2.73	4.34, −2.69	2.58, −1.93	7.41, −3.83

	250 K	325 K	375 K	425 K	475 K
Crystal data					
Chemical formula	Ag_7GeSe_5I	Ag_7GeSe_5I	Ag_7GeSe_5I	Ag_7GeSe_5I	Ag_7GeSe_5I
M_r	1349.4	1349.4	1349.4	1349.4	1349.4
Cell setting, space group	Cubic, $F\bar{4}3m$	Cubic, $F\bar{4}3m$	Cubic, $F\bar{4}3m$	Cubic, $F\bar{4}3m$	Cubic, $F\bar{4}3m$
Temperature (K)	250	325	375	425	475
a (Å)	11.0256 (4)	11.034 (5)	11.041 (4)	11.052 (10)	11.063 (7)
V (Å^3)	1340.3 (8)	1343.3 (11)	1345.9 (8)	1349.9 (5)	1354.0 (15)
Z	4	4	4	4	4
D_x (Mg m^{-3})	6.694	6.679	6.666	6.646	6.626
Radiation type	Mo $K\alpha$	Mo $K\alpha$	Mo $K\alpha$	Mo $K\alpha$	Mo $K\alpha$
μ (mm^{-1})	28.3	28.3	28.3	28.3	28.3
Crystal form, colour	Block, black	Block, black	Block, black	Block, black	Block, black
Crystal size (mm)	0.08 × 0.08 × 0.04	0.08 × 0.08 × 0.04	0.08 × 0.08 × 0.04	0.08 × 0.08 × 0.04	0.08 × 0.08 × 0.04
Data collection					
Diffractometer	Xcalibur-Sapphire 2	Xcalibur-Sapphire 2	Xcalibur-Sapphire 2	Xcalibur-Sapphire 2	Xcalibur-Sapphire 2
Data collection method	ω scans	ω scans	ω scans	ω scans	ω scans
Absorption correction	Numerical	Numerical	Numerical	Numerical	Numerical
T_{min}	0.21	0.21	0.21	0.21	0.21
T_{max}	0.46	0.46	0.46	0.46	0.46
No. of measured, independent and observed reflections	3491, 284, 230	3400, 260, 253	3747, 264, 255	4319, 266, 255	4318, 267, 256
Criterion for observed reflections	$I > 2\sigma(I)$	$I > 2\sigma(I)$	$I > 2\sigma(I)$	$I > 2\sigma(I)$	$I > 2\sigma(I)$
R_{int}	0.061	0.038	0.038	0.039	0.037
θ_{max} (°)	32.34	31.3	31.23	31.5	31.43

Table 1 (continued)

	250 K	325 K	375 K	425 K	475 K
Refinement					
Refinement on	F^2	F^2	F^2	F^2	F^2
$R[F^2 > 2\sigma(F^2)]$, $wR(F^2)$, S	0.058, 0.081, 2.92	0.041, 0.045, 6.72	0.045, 0.041, 6.95	0.039, 0.032, 5.25	0.043, 0.035, 6.10
No. of reflections	284	260	264	266	267
No. of parameters	37	37	39	39	39
Weighting scheme	Based on measured s.u.s, $w = 1/\sigma^2(I)$	Based on measured s.u.s, $w = 1/\sigma^2(I)$	Based on measured s.u.s, $w = 1/\sigma^2(I)$	Based on measured s.u.s, $w = 1/\sigma^2(I)$	Based on measured s.u.s, $w = 1/\sigma^2(I)$
$(\Delta/\sigma)_{max}$	0.024	0.006	0.017	0.030	0.022
$\Delta\rho_{max}$, $\Delta\rho_{min}$ (e Å^{-3})	1.40, −1.04	2.14, −0.95	1.57, −3.02	1.48, −0.98	0.77, −0.90

Computer programs used: *CrysAlis CCD* and *RED* (Oxford Diffraction, 2004), *SORTAV* (Blessing, 1989), *JANA*2000 (Petricek & Dusek, 2000), *ORTEP*III (Farrugia, 1997).

$A^{m+}_{(12-n/m)}B^{n+}X_6^{2-}$, where A is a monovalent (Ag, Cu) or divalent (Cd, Hg) cation, B is a trivalent (Ga), tetravalent (Si, Ge, Sn) or pentavalent (P, As) cation and X = S, Se, Te, were synthesized for the first time several decades ago (Hahn *et al.*, 1965; Kuhs *et al.*, 1979). Argyrodite materials often undergo a phase transition from a high-temperature superionic conducting phase, usually described as the γ form, to a low-temperature phase devoid of any superionic properties. The cubic γ-phase transition appears at 321 K for Ag_8GeS_6, 496 K for Ag_8GeSe_6 and 244 K for Ag_8GeTe_6 for example (Gorochov, 1968).

The argyrodite family can be extended if some of the chalcogenide anions are replaced by halides. The partially substituted halide argyrodites such as Ag_7GeX_5I (X = S, Se) do not show any phase transition, the γ cubic phase exists down to low temperature, at least that of liquid nitrogen (Cros *et al.*, 1988). Measurements on these materials revealed that the conductivity does not obey the Arrhenius law (Zerouale *et al.*, 1988; Ribes *et al.*, 1998; Belin, Zerouale, Pradel & Ribes, 2001). Such a deviation from the Arrhenius law is not unique and has already been reported for several superionic conductors (Mizuno *et al.*, 2006). The deviation is particularly noticeable at high temperature, where $\sigma \simeq 10^{-2}\ \Omega^{-1}\ cm^{-1}$. The plots for all the materials tend then towards the same limiting value for conductivity, *i.e.* that of α-AgI. Few explanations have been proposed to date for this particular behaviour. The free volume law (Vogel–Tammann–Fulcher law) could explain such a behaviour for Ag_7GeSe_5I (Zerouale *et al.*, 1988) and for $Li_{0.5}La_{0.5}TiO_3$ (Bohnke *et al.*, 2003). More recently, another explanation based upon a landscape model has been proposed (Mizuno *et al.*, 2006).

The conductivity behaviour could also have a structural basis. Since the halide-substituted argyrodite exhibits the cubic phase down to a very low temperature, both a change in conductivity and the structural evolution, including the occupation of silver sites and atomic displacement parameters, can be studied over a large temperature range.

The aim of the present work was to perform such a detailed temperature-dependent structural analysis: the structure of Ag_7GeSe_5I has been analyzed by single-crystal X-ray diffraction every 50 K in a temperature domain ranging from 15 to 475 K. This work complements a previous study carried out at two temperatures, 170 K and room temperature, and performed on two samples, a stoichiometric phase (Cros *et al.*, 1988) and a phase prepared by iodine vapour transport reaction and exhibiting a large deviation from stoichiometry ($Ag_{6.69}GeSe_5I_{0.69}$) (Zerouale *et al.*, 1988; Ribes *et al.*, 1998; Belin, Zerouale, Belin & Ribes, 2001).

2. Experimental

2.1. Synthesis

Prior to the synthesis of the substituted argyrodite, a batch of $GeSe_2$ was prepared by direct reaction of the elements Ge (Aldrich 99.99%) and Se (Aldrich 99.99%). The elements were mixed in stoichiometric proportions, placed in an evacuated fused silica tube and heated up to 873 K at the rate of 6 K h^{-1}, kept at this temperature for 3 d, then heated up to 1273 K for homogenization and slowly cooled down to room temperature. The crystallized product was orange–red.

The Ag_7GeSe_5I samples were further synthesized as follows: a mixture of Ag_2Se (Aldrich), $GeSe_2$ and AgI (Fluka 99%) in the proportions 3:1:1 + ε (excess AgI insured a complete reaction between the components) was placed in an evacuated fused silica tube. The tube was then heated up to 973 K at the rate of 8 K h^{-1} and maintained at this temperature for 1 d. It was then cooled down to 853 K, held at this temperature for a week and finally slowly cooled down to room temperature. The excess AgI was removed by washing the obtained powder in a KI solution. An X-ray diffraction pattern of the resulting samples did not reveal any crystallized impurity.

2.2. Thermal characterization

Thermal gravimetric analysis of the substituted argyrodite was carried out on a 2950 TGA HR V5.4A apparatus. The powder was heated up from 290 to 1273 K with a heating rate of 50 K min^{-1} in a nitrogen atmosphere. Cp measurements were performed from 80 to 420 K on a homemade apparatus as described in van Miltenburg *et al.* (1987).

2.3. Data collection and reduction

A single crystal of 80 × 80 × 40 μm^3 in size was selected from the powder and glued at the tip of a quartz capillary with araldite. The diffracted intensities were measured from 15 to 475 K on an Xcalibur2 four-circle diffractometer using Mo $K\alpha$ radiation (λ = 0.71069 Å, graphite monochromated) and a CDD area detector. An open-flow Helium cryosystem (Oxford Diffraction Helijet) was used for experiments from 15 to 70 K, while N_2 Cryojet equipment was used for the experiments at temperatures ranging between 100 and 298 K. High-temperature experiments were carried out with a hot-air blowing apparatus described in Argoud & Capponi (1984) and locally modified. For the latter, temperature was regulated within ± 3 K. The faces of the single crystal were indexed and the crystal shape empirically optimized based on the Bragg intensity of symmetry-equivalent reflections. A numerical absorption correction was performed using *CrysAlis* (Oxford Diffraction, 2004). Diffracted intensities were averaged in agreement with the symmetry of the noncentrosymmetric $F\bar{4}3m$ point group. Data reduction was carried out with the program *SORTAV* (Blessing, 1989). The maximum data resolution ranged from 31.2 to 39.1°. More details on data collection and reduction are given in Table 1.[1]

3. Results and discussion

3.1. Thermal characterization

The thermal stability of the argyrodite was first checked by thermogravimetry in order to validate the structural characterization over a large temperature range. The thermal stability domain of the argyrodite extends up to 620 K. At this temperature, a loss of matter starts and reaches 1.2 wt % at 673 K, as shown in Fig. 1.

The absence of a first-order phase transition over the temperature range 173–300 K, already shown in Cros *et al.* (1988), does not permit to discard the existence of a second-order phase transition. Such a transition could occur without any change in the crystal symmetry, but would be characterized by an increase in the entropy of the system and a maximum in the specific heat. Such transitions have already been observed in materials that show deviation from the Arrhenius law in their conductivity plots, *e.g.* $SrCl_2$ (Butman *et al.*, 2002; Carr *et al.*, 1978) or $RbAg_4I_5$ (Vargas *et al.*, 1977). The change in heat capacity with temperature for the argyrodite is shown in Fig. 2. No second-order phase transition can be detected in this curve that does not show any thermal event and obeys the Dulong and Petit law as expected (Dulong & Petit, 1819). The increase in heat capacity at high temperature could be the signature of some excess AgI that would not have been removed during the KI washing and would correspond to the $\beta \leftrightarrow \alpha$ transition at ∼ 420 K, or else could be related to the equipment limitation at this temperature.

[1] Supplementary data for this paper are available from the IUCr electronic archives (Reference: CK5029). Services for accessing these data are described at the back of the journal.

3.2. Structure

3.2.1. Literature survey. Many ternary argyrodites, $A^{m+}_{(12-n/m)}B^{n+}X^{2-}_6$ (A = Ag, Cu; B = Si, Ge, P; X = S, Se, Te), have been structurally characterized (Gorochov & Flahaut, 1967). The high-temperature superionic γ-phase of the argyrodites is usually cubic, but a structural description is difficult because of the inherent disorder that exists in the cation sublattice owing to the presence of many unoccupied crystallographic sites. The proper description of the electron density corresponding to the silver and copper cations is the main task in solving the structure. Often the most appropriate and physically meaningful model relies on a non-harmonic approximation of the atomic displacement parameters (ADPs; Boucher *et al.*, 1993).

The Ag_7PSe_6 and Cu_7PSe_6 argyrodites were characterized by Evain *et al.* (1998) and Gaudin *et al.* (2000). The disorder of silver and copper ions in the selenide environment was studied specifically. The high-temperature γ-Ag_7PSe_6 and γ-Cu_7PSe_6 forms were refined in agreement with the space group $F\bar{4}3m$ at 473 and 353 K, respectively. Three sites were proposed for

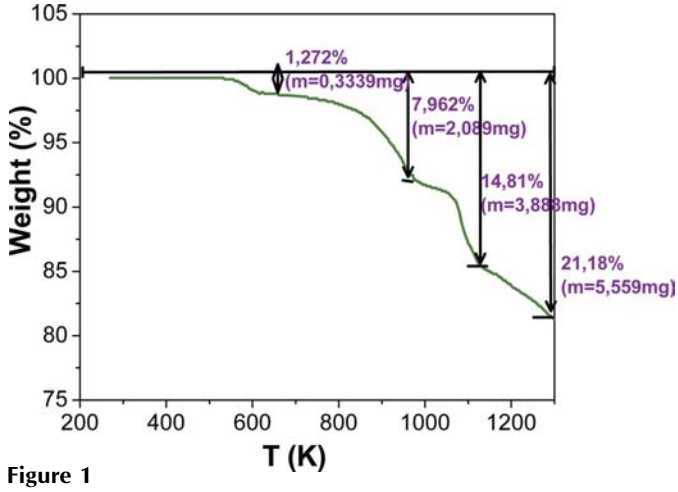

Figure 1
Thermogravimetric analysis of Ag_7GeSe_5I.

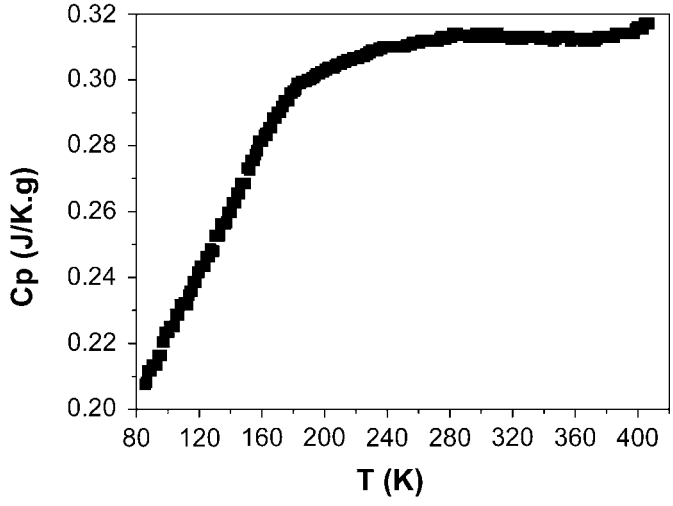

Figure 2
Evolution of specific heat with temperature for Ag_7GeSe_5I.

Table 2
Refinement details and results of the Hamilton significance test (at the 0.005 level) for the four models (T = 150 K).

Model B is significantly better than model A if $R_{\mathrm{mod}.B}(F)/R_{\mathrm{mod}.A}(F)$ is greater than $R_{b,n-m,0.005}$.

	Model # 1 High symmetry	Model # 2 Symmetry released	Model # 3 Anharmonicity	Model # 4 3 Ag
No. of unique data	284	284	284	284
No. of parameters	17	22	39	28
Observation criteria	$I > 2\sigma(I)$	$I > 2\sigma(I)$	$I > 2\sigma(I)$	$I > 2\sigma(I)$
$R(F)_{\mathrm{obs}}$ $[I > 2\sigma(I)]$	0.0991	0.0719	0.0465	0.0523
$R(F)_{\mathrm{all}}$ all data	0.1010	0.0733	0.0482	0.0542
GOF	2.78	1.91	2.28	2.61

	Model 1 → 2	Model 2 → 3	Model 4→3
Hamilton significance test for model $A \rightarrow B$ hypothesis			
$R_{\mathrm{mod}.B}(F)/R_{\mathrm{mod}.A}(F)$	1.378	1.521	1.124
b	5	17	11
$n - m$	262	245	245
$R_{b,n-m,0.005}$	1.032	1.074	1.056

silver and copper; the use of ADPs of third order, using Gram–Charlier expansion, improved the refinement considerably.

Several structural investigations of quaternary argyrodites with the chemical formula $A^{m+}_{(12-n/m)}B^{n+}X^{2-}_{(6-y)}Q^{-}_{y}$ (A = Ag, Cu; B = Si, Ge, P; X = S, Se; Q = Cl, Br, I) were also carried out. Ag^{+} quaternary argyrodites do not exhibit phase changes and crystallize in a cubic lattice, space group $F\bar{4}3m$. On the contrary, the cubic symmetry is only observed at high temperature in the case of copper argyrodites. Belin, Zerouale, Pradel & Ribes (2001) studied the structure of the non-stoichiometric substituted argyrodite $Ag_{6.69}GeSe_5I_{0.69}$. The refinements revealed a highly disordered structure with the Ag atoms distributed among two sites and anharmonic contributions to the silver and iodine atomic displacements. Nilges & Pfitzner (2005) investigated the structure of the $Cu^{m+}_{(12-n/m)}B^{n+}X^{2-}_{(6-y)}Q^{-}_{y}$ (B = P, As, Si; X = S, Se; Q = Cl, Br, I) compounds at room temperature for which the superionic behaviour was attributed to the order–disorder phenomena of the cation sublattice. In these latter materials, the Cu atoms are distributed among two or three sites, depending upon the specific compound considered, and the positions are always refined using a non-harmonic model.

3.2.2. Structural models for Ag_7GeSe_5I. The structure of the substituted argyrodite Ag_7GeSe_5I can be described as follows (Fig. 3): iodine and germanium are located on sites with multiplicity 4, *i.e.* 4(*a*) (0, 0, 0) and 4(*b*) ($\frac{1}{2}$, $\frac{1}{2}$, $\frac{1}{2}$), respectively. Se atoms are distributed over two sites: 16(*e*) (x, x, x), Se1 and Se2. Germanium is tetrahedrally coordinated by Se2 atoms. Ag atoms occupy two sites: 48(*h*) (x, x, z), Ag1 and Ag2. The structure involves a high disorder in the Se and Ag sublattices with 32 sites available for 20 Se and 96 sites for 28 Ag atoms in the unit cell (Cros *et al.*, 1988; Belin, Zerouale, Belin & Ribes, 2001).

Based upon the previous investigations, several strategies were used in order to determine the best structural model of the substituted argyrodite Ag_7GeSe_5I and especially the Ag sublattice. All structural refinements were carried out with the *JANA*2000 program (Petricek & Dusek, 2000), in agreement with the space group $F\bar{4}3m$ and based on reflections with $I > 2\sigma$.

Preliminary tests of refinement and Fourier syntheses indicated a high disorder in the iodine- and silver-ion positions with possible anharmonic contributions to the corresponding atomic displacements. Se1, which exhibits partial occupancy, was located within less than 0.3 Å from the high-symmetry position 4(*c*) ($\frac{1}{4}$, $\frac{1}{4}$, $\frac{1}{4}$), whereas Ag1 was close to 24(*g*) ($\frac{1}{4}$, $\frac{1}{4}$, z). Several structural models, including split-atom strategies or anharmonic expansions of the atomic displacements, have been defined and compared. The acceptability of the models was judged based on the values of the reliability factors R, wR and GOF, through the examination of difference-Fourier maps (residual electron density) and using Hamilton's significance tests (Hamilton, 1964, 1965). In the present situation, the anharmonic expansion of the atomic displacement factor was aimed at describing real anharmonicity but also accounts for atomic disorder effects. The different refinement models are described in details in the following, using the 150 K data set as an example. The main information is summarized in Table 2.

(i) In the first refinement model (model 1), all the atoms were located at their highest symmetry sites, *i.e.* maximum symmetry constraints were applied. The Ag atoms were distributed over two sites, *i.e.* Ag1 and Ag2, with refined complementary occupancies. ADPs were restricted to harmonic contributions (Kuhs, 1992).

(ii) The second model consisted of releasing the high-symmetry constraints for I, Se1 and Ag1. Nevertheless, iodine converged to the high-symmetry position (0, 0, 0) at the end of the refinement cycles; accordingly such an iodine 4(*a*) symmetry was kept in all further refinement models. Fourier synthesis at convergence of the second model exhibited high

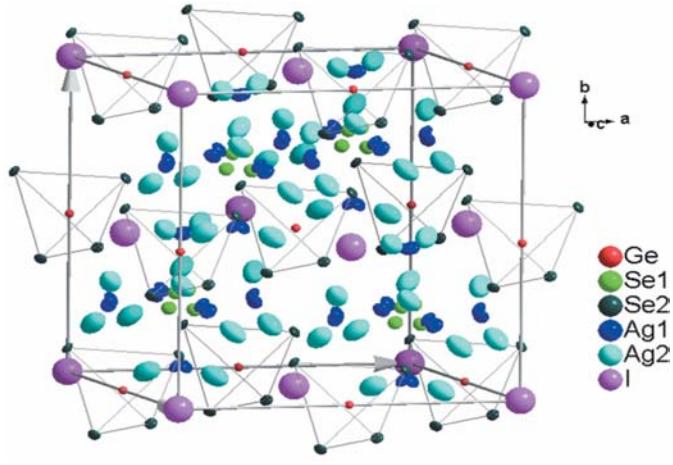

Figure 3
Cubic structure for Ag_7GeSe_5I.

Table 3
Final position and atomic displacement parameters U_{iso} (Å^2) from each data collection for Ag1 and Ag2.

		Occ. (%)	U_{iso}
15 K	Ag1	26.4 (1)	0.022 (1)
	Ag2	31.9 (1)	0.080 (2)
50 K	Ag1	27.2 (2)	0.0246 (6)
	Ag2	31.2 (2)	0.066 (2)
100 K	Ag1	26.0 (2)	0.0225 (9)
	Ag2	32.3 (2)	0.085 (3)
150 K	Ag1	28.2 (3)	0.041 (1)
	Ag2	30.2 (3)	0.088 (3)
200 K	Ag1	26.2 (3)	0.043 (1)
	Ag2	32.1 (3)	0.107 (3)
250 K	Ag1	22.2 (8)	0.028 (4)
	Ag2	36.1 (8)	0.144 (8)
325 K	Ag1	30.9 (2)	0.086 (1)
	Ag2	27.4 (2)	0.0124 (4)
375 K	Ag1	29.8 (3)	0.084 (1)
	Ag2	28.5 (3)	0.313 (6)
425 K	Ag1	32.8 (3)	0.152 (1)
	Ag2	25.6 (3)	0.278 (6)
475 K	Ag1	33.8 (4)	0.154 (2)
	Ag2	24.6 (4)	0.298 (8)

electron density residues close to I and Ag atoms, indicating possible anharmonic contributions.

(iii) In the third model, anharmonic terms of third and fourth orders in the Gram Charlier expansion were introduced for Ag2, while third and fifth order anharmonicity was considered for iodine. For the latter, fourth order terms had no significant values and did not improve the results; accordingly only odd orders were refined. Ag1 and Se1 were considered as in model II.

(iv) Model 4 was derived from model 3 using a split-atom hypothesis for Ag2 while retaining the harmonic approximation. The advantage of model 4 compared with model 3 is to keep the number of structural parameters as low as possible. Such an approach had already been proposed for the structural refinement of ternary argyrodites.

The results given in Table 2 clearly showed that model 1 was far too strict. High-symmetry positions for Se1 and Ag1 were not appropriate since releasing these symmetry constraints led to a large improvement of the agreement factors with only five more structural parameters. The corresponding Hamilton significance test was also very conclusive. In turn, model 2 was deficient in describing iodine and Ag2 electron densities. The introduction of 17 anharmonicity parameters in model 3 decreased $R(F)_{obs}$ by more than 2.5%. Note that at this point, we do not claim that the anharmonicity parameters account for real anharmonic behaviour. A complete discussion based on the evolution of these parameters *versus* temperature will be given in the section devoted to structural refinements. Treating Ag2 as harmonic but split over two positions (model 4) allowed the number of parameters to be as low as possible; but the agreement factors were slightly worse. Hamilton's significance test indicated that the improvement from model 4 to 3 was significant, at the expense of an 11 parameters increase. In addition, refinement instabilities were induced in model 4 by large correlations between Ag2 and Ag1 parameters. This complete refinement analysis led to the conclusion that the best model that we could achieve was model 3.

Depending on the temperature, and therefore on the structural behaviour, the model used for the refinement had to be optimized as follows. Except from 100 to 200 K, the iodine displacement parameters were restricted to a third-order anharmonicity, the introduction of fifth order did not improve the fit despite a physically meaningless increase in the number of model parameters. Ag2 was treated as anharmonic of the order 4, except at the lowest temperature (15 K) where it was restricted to third-order anharmonicity (R = 0.0596 for third order and R = 0.0623 for fourth order). At 100 K, the refined anisotropic displacement parameters for Ag1 lead to a non-positive definite ellipsoid (R = 0.0534 and GOF = 5.64); accordingly, Ag1 was described as isotropic even though the agreement factors slightly increased (R = 0.0550 and GOF = 5.72). At 15 K and above 250 K, Ag1 was described as anharmonic of the order 3 which led to a clear improvement in the model. The reliability factor then changed from 0.0474 down to 0.0407 at 325 K, from 0.0603 to 0.0442 at 375 K and from 0.0511 to 0.0387 at 425 K. However, the introduction of anharmonic ADP on Ag1 induced some correlations in the refinements, which encouraged us to restrict Se1 to isotropic ADP at 375 and 425 K.

The agreement factors obtained for all these models are of the same order of magnitude as those usually reported for similar structures (Hull *et al.*, 2001; Yoshiasa *et al.*, 1987). It is due to the possible inadequacy of an atomic analytical model to describe the observed electron density distribution in the case of high static and dynamic disorders and/or high anharmonic contributions to the atomic displacements. An R value of 0.0651 at 298 K for $Ag_{6.69}GeSe_5I_{0.69}$ was reported in Belin, Zerouale, Belin & Ribes (2001). Wada *et al.* (2002) gave a final agreement factor of 0.0480 at 298 K for Ag_8GeTe_6.

3.2.3. Structural analysis. The aim of this work was to find out whether the departure from the Arrhenius law in the 'conductivity *versus* temperature' plots could have a structural basis. It is clear that such anomalous behaviour occurs only in the high-temperature cubic form of the Ag^+ conducting argyrodites, which exhibits a strong disorder in the Ag^+ sublattice. The discussion that follows is based on the analysis of:

(i) the temperature dependence of the atomic harmonic and anharmonic displacement parameters and

(ii) the temperature dependence of the structural characteristics (coordination polyhedra and bond lengths).

The derived structural parameters related to the refinements have been deposited. The refined occupancies of the sites Ag1 and Ag2 are reported in Table 3. All distances with a physical meaning and smaller than 3.5 Å are given in Table 4.

3.3. Atomic structural parameters

The evolution of the cell parameter a with temperature, shown in Fig. 4, exhibited a continuous and linear behaviour over the large temperature range studied which confirmed the absence of any structural phase transition.

Table 4
Coordination and neighbour distances for the atoms of Ag_7GeSe_5I at each refinement temperature.

	Coord.	15 K	50 K	100 K	150 K	200 K	250 K	300 K	325 K	375 K	425 K	475 K
I	12 Ag2	2.511 (9)	2.586 (6)	2.599 (7)	2.544 (8)	2.569 (1)	2.58 (3)	2.634 (1)	2.577 (8)	2.407 (2)	2.411 (1)	2.403 (2)
Ge	4 Se2	2.352 (1)	2.356 (1)	2.349 (2)	2.360 (2)	2.356 (2)	2.374 (4)	2.347 (2)	2.350 (1)	2.341 (1)	2.342 (2)	2.350 (1)
Se1	3 Se1	0.868 (4)	0.817 (5)	0.834 (5)	0.794 (6)	0.746 (6)	0.684 (4)	0.607 (1)	0.597 (9)	0.47 (2)	0.4172 (2)	0.172 (2)
	3 Ag1	1.973 (3)	2.022 (4)	2.049 (5)	2.059 (8)	2.085 (6)	2.12 (2)	2.214 (1)	2.240 (8)	2.289 (2)	2.331 (4)	2.541 (7)
	3 Ag1	2.015 (3)	2.022 (4)	2.000 (5)	2.075 (8)	2.078 (6)	2.12 (2)	2.214 (1)	2.240 (8)	2.345 (2)	2.351 (4)	2.523 (7)
	6 Ag1	2.596 (3)	2.590 (4)	2.604 (5)	2.620 (8)	2.602 (6)	2.624 (2)	2.640 (1)	2.659 (8)	2.648 (2)	2.635 (4)	2.411 (7)
	3 Ag2	2.577 (9)	2.605 (9)	2.586 (9)	2.646 (1)	2.636 (1)	2.66 (2)	2.720 (2)	2.713 (2)	2.786 (2)	2.769 (1)	3.15 (2)
	3 Ag2	2.989 (9)	2.982 (8)	2.970 (9)	3.022 (1)	2.985 (1)	2.98 (2)	2.990 (2)	2.990 (1)	3.030 (2)	2.987 (1)	3.07 (2)
	6 Ag2	3.337 (9)	3.317 (9)	3.313 (9)	3.340 (1)	3.287 (1)	3.26 (2)	3.246 (2)	3.233 (2)	3.200 (2)	3.135 (1)	3.00 (2)
Se2	1 Ge	2.352 (1)	2.705 (7)	2.349 (2)	2.360 (2)	2.356 (2)	2.374 (4)	2.347 (2)	2.350 (2)	2.341 (2)	2.342 (1)	2.350 (1)
	6 Ag1	2.689 (1)	2.676 (2)	2.681 (6)	2.662 (1)	2.662 (3)	2.650 (13)	2.624 (5)	2.602 (3)	2.605 (4)	2.584 (3)	2.610 (5)
	6 Ag2	2.729 (9)	2.705 (7)	2.710 (8)	2.736 (9)	2.741 (1)	2.75 (2)	2.727 (1)	2.761 (1)	2.890 (1)	2.923 (1)	2.90 (2)
Ag1	1 Se1	1.973 (3)	2.022 (4)	2.049 (5)	2.059 (8)	2.078 (6)	2.12 (2)	2.214 (1)	2.240 (8)	2.289 (2)	2.331 (4)	2.541 (7)
	1 Se1	2.015 (3)	2.022 (4)	2.000 (5)	2.075 (8)	2.085 (6)	2.12 (2)	2.214 (1)	2.240 (8)	2.345 (2)	2.351 (4)	2.523 (7)
	2 Se1	2.596 (3)	2.59 (4)	2.604 (5)	2.620 (8)	2.602 (6)	2.66 (2)	2.640 (1)	2.659 (8)	2.648 (2)	2.635 (5)	2.411 (7)
	2 Se2	2.689 (1)	2.676 (2)	2.681 (6)	2.662 (1)	2.662 (3)	2.650 (13)	2.624 (5)	2.602 (3)	2.605 (4)	2.584 (3)	2.61 (5)
	2 Ag1	3.0867 (2)	3.209 (2)	3.332 (8)	3.223 (2)	3.287 (4)	3.14 (2)			3.201 (5)		3.218 (7)
	2 Ag2	3.089 (8)	3.191 (8)	3.283 (1)	3.179 (2)	3.178 (1)	3.05 (3)	3.268 (1)	3.224 (1)	2.956 (2)	3.053 (1)	2.97 (2)
Ag2	1 I	2.551 (9)	2.586 (6)	2.599 (7)	2.544 (8)	2.569 (1)	2.58 (3)	2.634 (1)	2.577 (8)	2.407 (2)	2.411 (1)	2.403 (2)
	1 Se1	2.577 (9)	2.605 (9)	2.586 (9)	2.646 (1)	2.636 (1)	2.66 (2)	2.720 (2)	2.713 (2)	2.786 (2)	2.769 (1)	3.15 (2)
	1 Se1	2.989 (9)	2.982 (8)	2.970 (9)	3.022 (1)	2.985 (1)	2.98 (2)	2.990 (2)	2.990 (1)	3.030 (2)	2.987 (1)	3.07 (2)
	2 Se2	2.729 (9)	2.705 (7)	2.710 (8)	2.736 (9)	2.741 (1)	2.75 (2)	2.727 (1)	2.761 (1)	2.890 (1)	2.923 (1)	2.90 (2)
	2 Ag1	3.089 (8)	3.191 (8)	3.283 (0)	3.179 (2)	3.178 (1)	3.05 (3)	3.268 (1)	3.244 (1)	2.956 (9)	3.053 (1)	2.97 (2)
	2 Ag2	2.53 (1)	2.587 (1)	2.586 (1)	2.550 (1)	2.534 (1)	2.52 (3)	2.625 (2)	2.527 (2)	2.248 (2)	2.169 (2)	2.24 (3)
	1 Ag2	2.645 (3)	2.577 (9)	2.558 (1)	2.684 (1)	2.636 (1)	2.64 (4)	2.545 (1)	2.648 (1)	3.00 (2)	3.005 (2)	3.02 (3)
	2 Ag2	2.570 (1)	2.586 (1)	2.612 (1)	2.537 (1)	2.605 (1)	2.63 (3)	2.644 (2)	2.628 (2)	2.560 (2)	2.642 (2)	2.56 (3)

The analysis of the Debye–Waller factor, B_{iso}, as well as the evolution of the anharmonic parameters *versus* temperature was very informative. The first step was to compare the B_{iso} values (Å^2) found in the present work with those reported in the literature for the most studied and most representative superionic phases, *i.e.* α-Ag_3SI (Keen & Hull, 2001; Hull *et al.*, 2001), γ-Ag_8GeTe_6 (Boucher *et al.*, 1993), γ-Ag_7PSe_6 (Gaudin *et al.* 2000), $RbAg_4I_5$ (Hull *et al.*, 2002) and α-AgI (Bürher & Hälg, 1974; Wright & Fender, 1977). B_{iso} values for the Ag^+ sites ranged between 4.5 and 23 Å^2 for temperatures ranging from 298 to 723 K. On the whole, the values are largely dispersed. However, they all indicate the same positive trend, the highest B_{iso} being reported for the highest measurement temperatures. The B_{iso} values found for the substituted argyrodite (Table 3) are in the same range as the literature ones: B_{iso} for Ag1 changes from 1.7 to 12.2 Å^2 and B_{iso} for Ag2 from 6.3 to 23.5 Å^2 when T increases from 15 to 475 K. The atomic displacement parameters for Ag^+ in such ionic conductors are clearly the signature of extensive static and dynamic disorder. As for iodine, B_{iso} changes very slightly from 7.3 to 8.4 Å^2 when T increases from 15 to 475 K. These B_{iso} values agree fairly well with the values found in the literature: they range from 4.2 to 11 Å^2 for T between 298 and 723 K.

The temperature dependence of the Debye–Waller factor B_{iso}(Å^2) for all atoms is depicted in Fig. 5. Since B_{iso} accounts for all the vibration modes of the atom considered, it should globally decrease with temperature and should tend to an almost constant value corresponding to the zero-point vibration at very low temperature. Such an expected behaviour was indeed observed for most of the atoms of the structure, *i.e.* Se1, Se2, Ge and both Ag atoms either located on site Ag1 or on site Ag2. On the contrary, unusual behaviour was observed for iodine with a high displacement amplitude that did not depend significantly on temperature: U^{11} = 0.093 (2) at 15 K and 0.107 (2) at 425 K, and corresponds to a B_{iso} value of $\sim$ 8 Å^2 over the whole temperature range. It is a clear indication that iodine exhibits a high static disorder centered on its

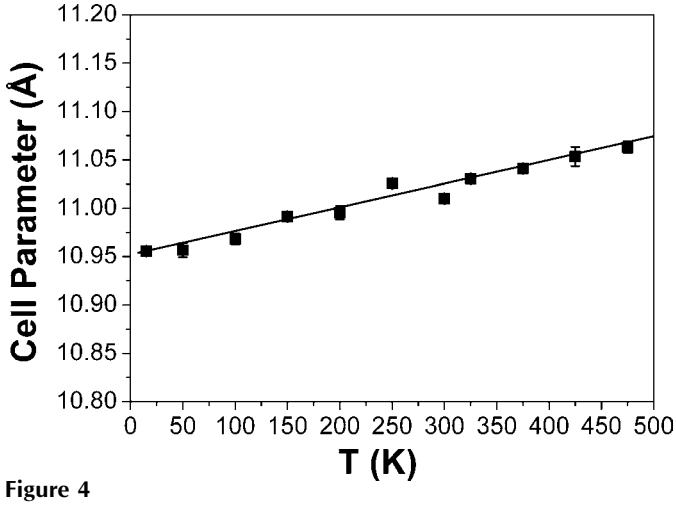

Figure 4
Evolution of the cell parameter with temperature for Ag_7GeSe_5I.

mean position (0,0,0). Such a strong disorder has been efficiently accounted for by using anharmonic terms in the structural refinement, which obviously does not correspond to a real anharmonic behaviour. On the other hand, Ge and Se2 atoms that form the $GeSe_4$ tetrahedra show expected Debye behaviour with a quasi-constant B_{iso} value at low temperature and a quasi-linear increase in B_{iso} at higher temperature. Se1 follows the same trend up to 300 K. The deviation at higher temperature is probably due to a contribution of disorder. The Ag2 and Ag1 sites have large Debye–Waller factors that increase with temperature. Ag2 has the highest B_{iso}, *i.e.* 6.29 (39) Å^2 at 15 K to be compared with 1.71 (18) Å^2 for Ag1 at the same temperature. The Debye–Waller factors for silver behaved differently from those of all the other atoms of the framework. In fact, while the latter factors showed a smooth increase with temperature, the silver B_{iso} increased strongly at the highest temperatures after a transition domain ranging from 250 to 300 K.

The parameters of the structural refinements indicated a systematic trend in the complementary refined occupancies of the two Ag sites. Up to 250 K, the occupancy of Ag1 [22.2 (8)–28.2 (3)%] is clearly lower than Ag2 [36.1 (8)–30.2 (3)%]. From 325 K, an inversion in the occupancy of the two silver sites occurred (Table 3), indicating a partial transfer from site 2 to 1 setting up around 300 K.

3.4. Structural analysis

The substituted argyrodite Ag_7GeSe_5I structure can be described as a framework of individual I^-, Se^{2-} and $GeSe^{4-}$ anions with Ag^+ ions distributed over two sites in the voids of the structure (Fig. 3). By comparison, in the first description by Cros *et al.* (1988), three sites were identified for silver. The structure of the previously studied non-stoichiometric phase $Ag_{6.69}GeSe_5I_{0.69}$ (Belin, Zerouale, Belin & Ribes, 2001) was very similar to that found in the present study. The main difference lay in the occupancy of the 4(*a*) site by iodine. While the occupancy was only 69% for the non-stoichiometric phase, full occupancy was found here.

As shown in Fig. 6, iodine occupies the centre of a cuboctahedron statistically formed by 12 Ag2 with an occupancy ratio changing from 31.9% at 15 K to 24.6% at 475 K. No Ag1 is found in the iodine environment. Se1 has a strong ionic character (Se^{2-}); it is located at the centre of a truncated Friauf polyhedron, built from 12 Ag1 sites and 12 Ag2 sites, the first ones being closer to the selenium position than the second (Fig. 7). The distortion of this polyhedron tends to decrease with increasing temperature. Germanium is the centre of a perfect tetrahedron formed by Se2 atoms. The distance Ge—Se2 changes only slightly with temperature, the shortest [2.341 (1) Å] and longest [2.374 (4) Å] distances being observed at 375 and 250 K, respectively. The triangular environment of Ag^+ ions located at site Ag1 is strongly distorted at low temperature with two families of Ag1—Se distances, one being close to 2 Å and the other in the range 2.6–2.7 Å (Fig. 8). The environment is much more regular at high temperature with all Ag1—Se distances equal to 2.5 Å within 0.1 Å. The change is mainly due to a continuous increase in two of the Ag1—Se1 distances with temperature. The existence of four different Ag1—Se1 distances is the consequence of the Se1 positional disorder close to the high-symmetry position 4(*c*) ($\frac{1}{4}$, $\frac{1}{4}$, $\frac{1}{4}$). The Ag2 site is located at the centre of a distorted tetrahedron which consists of an I atom, two Se2 and one Se1. At low temperature, the Ag2—I and Ag2—Se distances are dispersed from 2.551 (9) to 2.989 (9) Å, while at higher temperatures, the Ag—I bond becomes clearly shorter (~ 2.4 Å) than the three Ag—Se bonds (~ 3 Å), as depicted in Fig. 9. The triangular environment for Ag1 becomes more and more regular with increasing temperature, whereas the opposite situation occurs for the Ag2 tetrahedron.

The Ag atoms located at distances between 2.2 and 3.5 Å from Ag1 and Ag2 sites may also weakly contribute to the corresponding coordination polyhedron. d^{10} ions can indeed induce a weak hybridization, 5*s* 4*d*, as already reported in

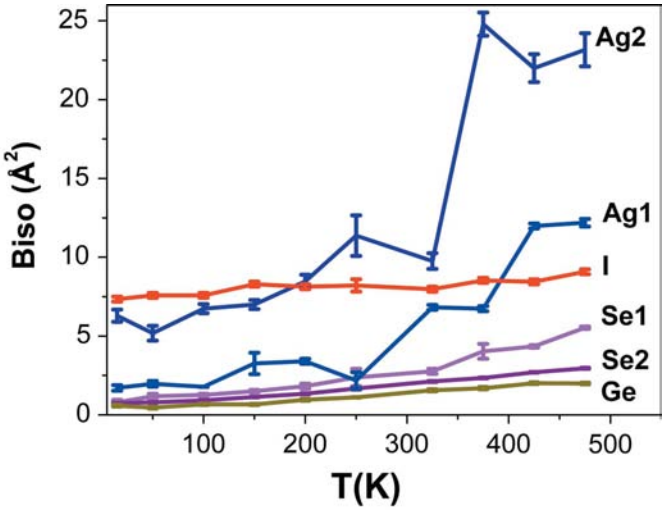

Figure 5
Evolution in Debye Waller factors as a function of temperature for all sites.

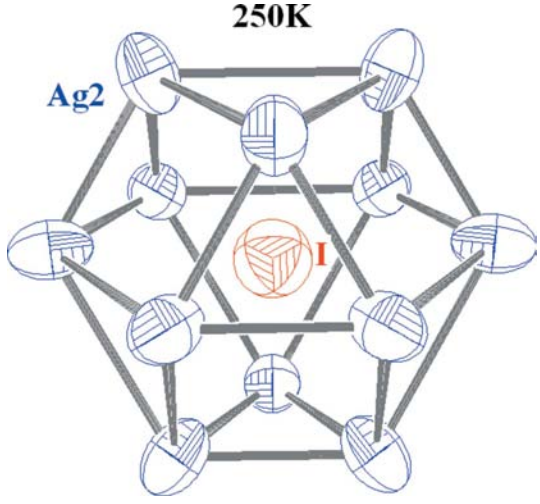

Figure 6
Ag coordination polyhedron for iodine at 250 K.

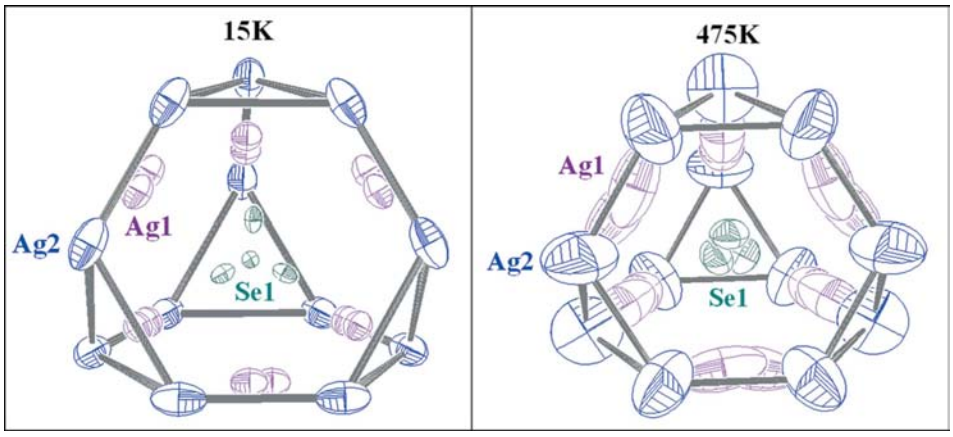

Figure 7
Ag coordination polyhedron for Se1 at 15 and 475 K.

Gaudin *et al.* (2000). A weak hybridization, $5s^{0.03}$ $4d^{9.97}$, was also found in the case of the non-stoichiometric argyrodite (Belin, Zerouale, Belin & Ribes, 2001). Such very weak interactions have an anti-bonding and repulsive character when the distances are smaller than 2.2 Å, but are slightly bonding for distances between 2.2 and 3.5 Å with a maximum at 3.5 Å. Note that the Ag—Ag distances in Ag^0 metal are 2.89 Å.

3.5. Possible diffusion pathways

In order to obtain a better insight into the mobility of silver throughout the crystal lattice, the Ag^+ joint probability density function (j.p.d.f.) was analyzed (Kuhs, 1983). Such an inspection might help in identifying diffusion pathways for the mobile Ag^+ ions in the voids of the I, Se and $GeSe_4$ framework. Data are given in Fig. 10. At 15 K, the j.p.d.f. exhibits well localized maxima corresponding to Ag1 and Ag2 atomic positions. On increasing the temperature, the separated maxima are gradually smeared out, indicating that the Ag ions are more and more delocalized. At the highest temperature of 475 K, the maxima can no longer be distinguished from one another. As a matter of fact, the j.p.d.f. can be visualized as a continuum from nearly 300 K (see Fig. 11). This general evolution is consistent with the large increase in Ag1 and Ag2 atomic displacement parameters described above. Accordingly, such parameters should not be too rigorously considered as true displacement amplitudes, but rather as a combination of displacement amplitudes and multiple atomic positions (disorder). The temperature when the continuum for j.p.d.f. is observed also corresponds to the temperature at which the occupancy inversion between Ag1 and Ag2 was observed.

On the whole, these results point towards an environment for silver which changes and becomes more favorable to its mobility.

4. Conclusion

The conductivity of the solid superionic conductors and its very low activation energy are very similar to those of the best electrolytic solutions. The mobile ions are generally d^{10} ions, Ag^+ or Cu^+. The large conductivity is usually only observed in the high-temperature cubic phases where a strong disorder in the mobile ion sublattice exists. The family of Ag^+-substituted argyrodites has a particular place in this class of materials

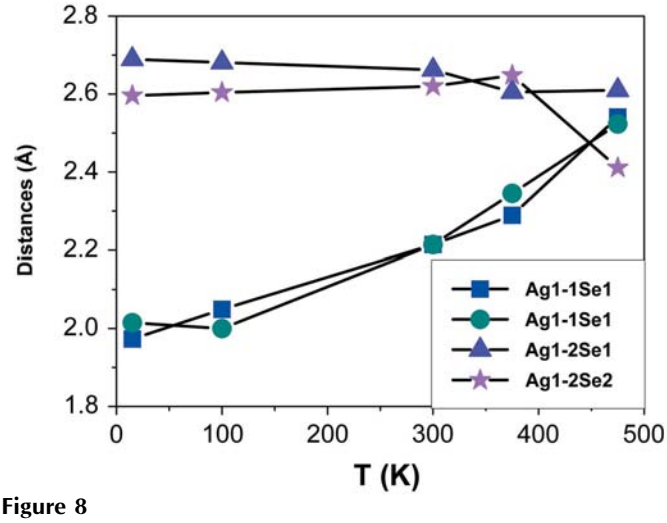

Figure 8
Evolution in Ag1—Se distances as a function of temperature in the triangular environment of Ag1.

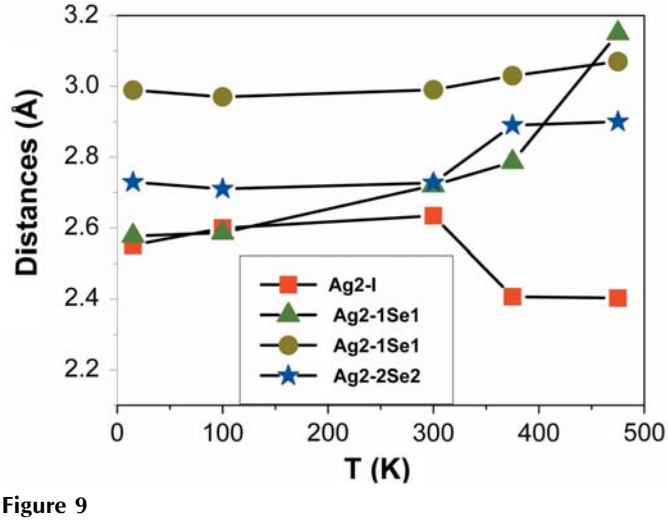

Figure 9
Evolution in Ag2—Se and Ag2—I distances as a function of temperature in the tetrahedral environment of Ag2.

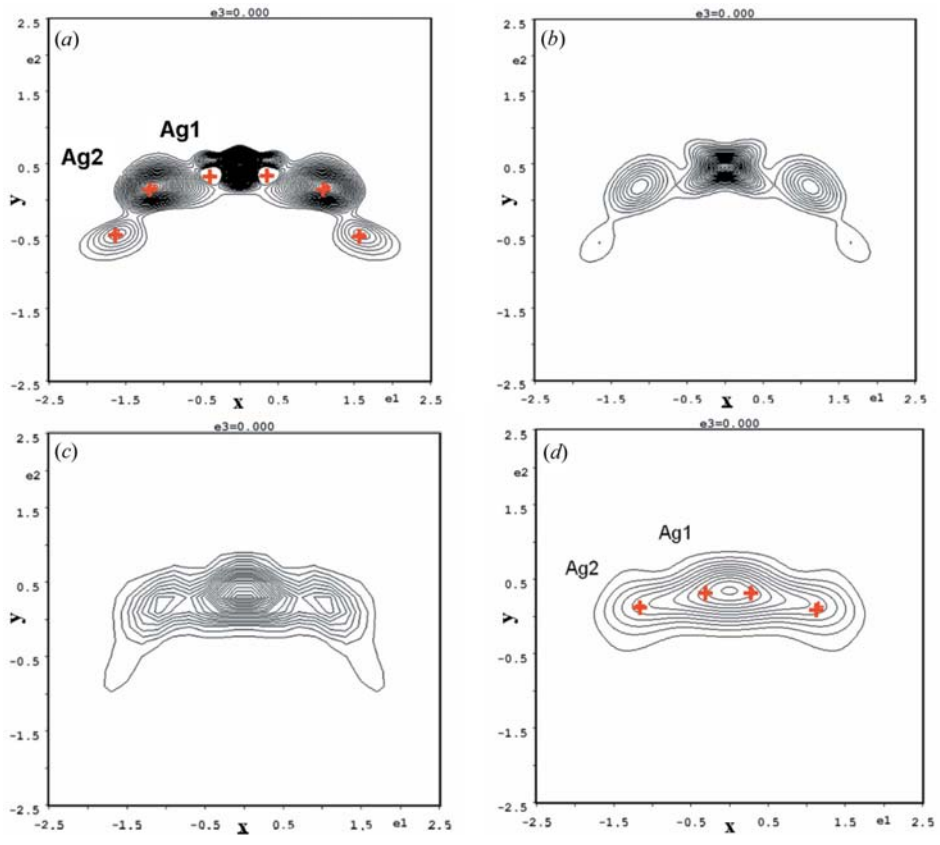

Figure 10
Probability density function of silver along the direct jump pathway between two faces sharing tetrahedra for Ag_7GeSe_5I. Section defined by the Ag1 and Ag2 positions (indicated by crosses) (*a*) at 15 K, (*b*) at 150 K, (*c*) at 325 K and (*d*) at 475 K. Contours lines: 0.2–10.5 Å^{-3}.

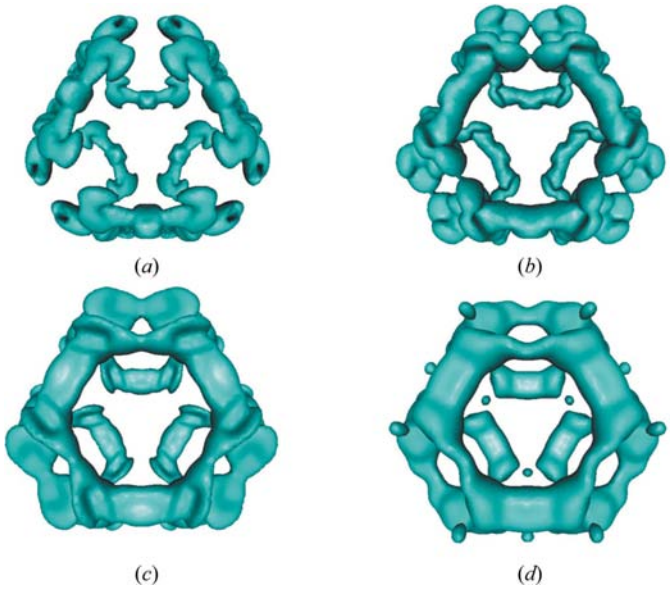

Figure 11
Isosurface (0.035 level) of the joint probability density viewed along the [111] direction at (*a*) 15, (*b*) 150, (*c*) 325 and (*d*) 475 K (Ag1 and Ag2 alone are included).

since the cubic phase then exists in the whole temperature range.

The present work reports on an investigation of the cubic phase Ag_7GeSe_5I that crystallizes in the space group $F\bar{4}3m$. Structural characterization was carried out at ten different temperatures in steps of 50 K from 15 to 475 K. The main goal was to look for possible correlations between the unusual conductivity behaviour, *i.e.* a deviation from the Arrhenius law, and the structural evolution as a function of temperature.

The main difficulty and task in solving and describing the structure of the argyrodite was to define an efficient model for the distribution of the heavily disordered silver ions. These latter ions are highly mobile and responsible for the conductivity properties. Accordingly, a temperature dependence of their positions and thermal displacements was expected. The best structural model we could achieve consisted of two main occupied sites, Ag1 and Ag2, with anharmonic contributions to the atomic displacement parameters. Ag1 has a distorted triangular environment which becomes more and more regular as temperature increases, while Ag2 is a distorted tetrahedral environment which becomes more and more distorted with temperature. The remaining structure, which consists of a framework of I, Ge, Se and $GeSe_4$ ionic units, is only partially affected by static disorder which is accounted for using an anharmonic model for I.

Very large values for B_{iso} of I and Ag2 were found at very low temperatures. Could it be an explanation for the existence of the cubic phase down to the low temperature or is it a consequence of its existence? The question is still pending.

A strong increase in the B_{iso} values for the sites Ag1 and Ag2 at the highest temperatures and an inversion in the occupation ratio of the two sites (partial transfer from Ag2 to Ag1) at about 300 K were observed. On the whole, a larger and larger delocalization of silver, revealed on the joint probability density function, was observed with increasing temperature, which agrees with the non-Arrhenius behaviour of conductivity in the AgI-substituted argyrodite.

The authors thank Professor J. C. van Miltenburg from the Chemical Thermodynamics Group of Utrecht University, The Netherlands, for the Cp measurements of the argyrodite.

References

Argoud, R. & Capponi, J. J. (1984). *J. Appl. Cryst.* **17**, 420–425.
Belin, R., Zerouale, A., Belin, C. & Ribes, M. (2001). *Solid State Sci.* **3**, 251–265.
Belin, R., Zerouale, A., Pradel, A. & Ribes, M. (2001). *Solid State Ion.* **143**, 445–455.
Blessing, R. H. (1989). *J. Appl. Cryst.* **22**, 396–397.
Bohnke, O. J., Emery, J. & Fourquet, J. L. (2003). *Solid State Ion.* **158**, 119–132.
Boucher, F., Evain, M. & Brec, R. (1993). *J. Solid State Chem.* **107**, 333–346.
Bürher, W. & Hälg, W. (1974). *Rapport de la Session d'Automne de la Société Suisse de Physique*, Vol. 47.
Butman, M. F., Smirnov, A. A., Kudin, L. S. & Dabringhaus, H. (2002). *Surf. Sci.* **511**, 331–339.
Carr, V. M., Chadwick, A. V. & Saghafian, R. (1978). *J. Phys. Solid State Phys.* **11**, L637–L641.
Cros, B., Zerouale, A., Pintard, M., Philippot, E. & Ribes, M. (1988). *Eur. J. Solid State Inorg. Chem.* **25**, 541–549.
Dulong, P. & Petit, A. (1819). *Ann. Chim. Phys.* **10**, 395–413.
Evain, M., Gaudin, E., Boucher, F., Petricek, V. & Taulelle, F. (1998). *Acta Cryst.* B**54**, 376–383.
Farrugia, L. J. (1997). *J. Appl. Cryst.* **30**, 565.
Gaudin, E., Boucher, F., Petricek, V., Taulelle, F. & Evain, M. (2000). *Acta Cryst.* B**56**, 402–408.
Gorochov, O. (1968). *Bull. Soc. Chim.* **6**, 2263–2274.
Gorochov, O. & Flahaut, J. (1967). *C. R. Acad. Sci. Paris*, **264**, 2153–2155.
Hahn, H., Schulze, H. & Sechser, L. (1965). *Naturwissenschaften*, **52**, 451.
Hamilton, W. C. (1964). *Statistics in Physical Science.* New York: Ronald Press Company.
Hamilton, W. C. (1965). *Acta Cryst.* **18**, 502–510.
Hull, S., Keen, D. A., Gardner, N. J. & Hayes, W. (2001). *J. Phys. Condens. Matter*, **13**, 2295–2316.
Hull, S., Keen, D. A., Sivia, D. S. & Berastegui, P. (2002). *J. Solid State Chem.* **165**, 363–371.
Keen, D. A. & Hull, S. (2001). *J. Phys. Condens. Matter*, **13**, L343–L347.
Kuhs, W. F. (1983). *Acta Cryst.* A**39**, 148–158.
Kuhs, W. F. (1992). *Acta Cryst.* A**48**, 80–98.
Kuhs, W. F., Nitsche, R. & Scheunemann, K. (1979). *Mater. Res. Bull.* **14**, 241–248.
Mahan, G. D. & Roth, W. L. (1976). *Superionic Conductors.* New York: Plenum Press.
Miltenburg, J. C. van, van den Berg, G. J. K. & van Bommel, M. J. (1987). *J. Chem. Thermodyn.* **19**, 1129–1137.
Mizuno, F., Belieres, J. P., Kuwata, N., Pradel, A., Ribes, M. & Angell, C. A. (2006). *J. Non-Cryst. Solids*, **352**, 5147–5155.
Nilges, T. & Pfitzner, A. (2005). *Z. Kristallogr.* **220**, 281–294.
Oxford Diffraction (2004). *CrysAlis*, Version 1.171. Oxford Diffraction, Wroclaw, Poland.
Petricek, V. & Dusek, M. (2000). *JANA*2000. Institut of Physics, Praha, Czech Republic.
Ribes, M., Taillades, G. & Pradel, A. (1998). *Solid State Ion.* **105**, 159–165.
Vargas, R. A., Salamon, M. B. & Flynn, C. P. (1977). *Phys. Rev.* B**17**, 269–281.
Wada, H., Sato, A., Onoda, M., Adams, S., Tansho, M. & Ishii, M. (2002). *Solid State Ion.* **154–155**, 723–727.
Wright, A. F. & Fender, B. E. F. (1977). *J. Phys. Solid State Phys.* **10**, 2261–2267.
Yoshiasa, A., Koto, K., Kanamaru, F., Emura, S. & Horiuchi, H. (1987). *Acta Cryst.* B**43**, 434–440.
Zerouale, A., Cros, B., Deroide, B. & Ribes, M. (1988). *Solid State Ion.* **28–30**, 1317–1319.